Aquaculture 576 (2023) 739859

Contents lists available at ScienceDirect

Aquaculture

journal homepage: www.elsevier.com/locate/aquaculture

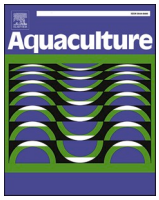

The skin structure in multiple color variants of barramundi (*Lates calcarifer*): A histological, immunohistochemical and ultrastructural overview

R. Marcoli [b,*], D.B. Jones [a,b], C. Massault [a,b], A.F. Marc [b], M. Moran [b], P.J. Harrison [a,e], H.S. Cate [a,e], A.L. Lopata [a,b,c,d], D.R. Jerry [a,b,c]

[a] *ARC Research Hub for Supercharging Tropical Aquaculture through Genetic Solutions, James Cook University, QLD, Australia*
[b] *Centre for Sustainable Tropical Fisheries, College of Science and Engineering, James Cook University, Townsville, QLD, Australia*
[c] *Tropical Future Institute, James Cook University, Singapore*
[d] *Australian Institute of Tropical Health & Medicine, Centre for Molecular Therapeutics, Centre for Sustainable Tropical Fisheries and Aquaculture, Australia*
[e] *Mainstream Aquaculture Group Pty Ltd, Werribee, VIC 3030, Australia*

ARTICLE INFO

Keywords:
Aquaculture
Lates calcarifer
Asian seabass
Fish
Skin structure
Color variants
TEM
Immunohistochemistry
Melanophores
Histology

ABSTRACT

Barramundi (*Lates calcarifer*), a popular aquaculture species, has silver to bronze skin coloration with rare golden, "panda" (golden and black spots), and black variants. Increased production of these rare color variants is commercially desirable; however, the differences in skin-cell morphologies have not been characterized. Microscopy, transmission electron microscopy, and immunohistochemistry were utilized to characterize morphological, ultrastructural, and cellular differences between barramundi color variants. Notably, melanophores, iridophores, and xanthophores were evident. Differences in the occurrence of melanin were visible, with a reduction in melanophores in the golden (average of 0.47 melanophores/cm^2) versus the silver (average of 218.6 melanophores/cm^2) or black (average of 462.9 melanophores/cm^2) color phenotypes. Furthermore, a significant decrease in melanophores was observed in panda variant at the edge between golden and black patches: golden vs. edge ($p < 0.001$), golden vs. black ($p < 0.001$) and edge vs. black ($p < 0.001$). The TEM analysis revealed a distinct difference in melanophores and mature melanosomes, with stages 1, 2, 3, and 4 melanosomes present in silver variants and rare stage 1 (immature) melanosomes in golden variant. Furthermore, the immunohistochemical techniques provided independent and thorough documentation of the presence and maturity of melanophores and melanosomes across highly valued barramundi color variants. In conclusion, the color of barramundi appears to be driven by the presence/absence and number of melanophores in the skin layer.

1. Introduction

Barramundi (*Lates calcarifer*) is a commercially important aquaculture and capture-fishery species throughout its tropical Indo-Pacific distribution (Jerry, 2013). Skin coloration in barramundi commonly varies from silver to bronze; however, rare golden (xanthic), panda (barramundi with golden and black patches), and black color variants are occasionally found (Fig. 1).

Golden skin-colored barramundi are valuable for the aquarium trade, but most significantly, from a farming perspective, golden variants do not exhibit the intensity of "greying" of the flesh, which is a negative consumer attribute often found in farmed barramundi fillets. Golden skin coloration (or xanthism) has been described in numerous other aquaculture finfish species (Dunham and Childers, 1980; Huang et al., 2021; Lewand et al., 2013; Pathan, 2022; Pawar and Jawad, 2017) and has been identified as a desirable attribute for the market, making this color trait particularly appealing for the Australian barramundi aquaculture industry. Despite the commercial importance of skin and flesh coloration in this species, no studies have described attributes of the skin and particularly the dispersion of pigment-producing cells among the different colored variants. Elucidation of differences within the skin that may be present among the color variants is the first step in not only understanding pigmentation of barramundi, but also giving insights into possible genetic and/or environmental drivers of coloration

* Corresponding author.
E-mail address: roberta.marcoli@jcu.edu.au (R. Marcoli).

https://doi.org/10.1016/j.aquaculture.2023.739859
Received 12 February 2023; Received in revised form 29 June 2023; Accepted 1 July 2023
Available online 5 July 2023

in this species.

In teleosts, cellular, genetic, and physiological factors all play a role in determining skin coloration (Colihueque, 2010). At a cellular level, coloration is dependent on interactions among pigment-producing cells, also called chromatophores (Burton, 2011). In finfish, multiple chromatophore cell-types have been characterized which contain pigments that each selectively absorb or reflect particular wavelengths of light (Burton, 2002). These chromatophore cell-types differ in their presence within teleosts, with the most common cell-types being (i) melanophores that are light absorbing, dendritic cells, comprising intra-cellular melanin-producing organelles called melanosomes (Cal et al., 2017); ii) iridophores that are iridescent/silver pigmented cells able to reflect light through the presence of purine platelets (Kelsh, 2004); iii) xanthophores that are yellow pigment-producing cells, characterized by the presence of xanthosomes, organelles containing pteridine and carotenoids pigments absorbing blue light (Burton, 2011), and iv) erythrophores that are characterized by erythrosomes, containing carotenoids (Burton, 2011). Commonly, chromatophores in fish skin appear to be predominantly in the upper layer of the dermis, but they have also been reported in the epidermal layer (Elliott, 2011); the quantity, dispersion, and location of chromatophores in the fish skin is thought to determine the final coloration of the animal (Nilsson Sköld et al., 2013). In addition, extrinsic environmental variables such as temperature, dissolved oxygen (and especially hypoxia), background color, and light cycles also have a noticeable effect on the color of the skin (Dong et al., 2011; Estlander et al., 2010; Kalinowski et al., 2007; Segade et al., 2015). Those changes are normally correlated with reduction in melanophore number, changes in melanin production, or the dispersion of melanosomes in the melanophores (Leclercq et al., 2010), through activation of pathways that involve cell survival, melanin formation and dispersion (Leclercq et al., 2010).

This study investigated the differences in cellular composition and structure of the skin and fin in four barramundi color variants, through the utilization of histological, immunohistochemical, and ultrastructural techniques. In particular, understanding the morphological and physiological changes that occur in the golden color variants is the first step in identifying the mechanisms underlying skin color, which in turn permits targeted practices to be applied by the industry that could result in higher proportions of farmed golden variants.

2. Material and methods

2.1. Fish

All fish used in this study came from a commercial hatchery (Mainstream Aquaculture Group, Werribee, Australia) and were housed in a 2000-liter tank that is part of a 10-tank recirculating tank system. Three times per week, the fish were fed commercial aquaculture feed to satiety. The animals were closely monitored during feeding and routinely inspected throughout the day, with all mortalities being removed from the tanks and weighed. The photoperiod was set to correspond with daylight, with lights off at night. For tissue analyses, $n = 22$ barramundi (weight: 0.618 ± 0.09 kg, length: 345.14 ± 10.96 cm, with ± representing standard error) were weighed using a digital balance and their lengths were measured to the nearest mm using a ruler and tape measure. The fish were euthanized in a bath containing 40 mg/L of isoeugenol (Aqui-S®, New Zealand Ltd.), after which spinal dislocation was performed (JCU Animal ethics approval: A2829).

2.2. Light microscopy

Approximately 3 cm^3 of skin tissue (subsequently divided into two pieces) was excised from the dorsal fin, along with the shoulder (dorsal) and belly (ventral) of the fish. Since "panda" variants exhibit black and golden colored patches, two tissue samples were collected from each of this colored variant encompassing both golden- and black-pigmented regions. Samples were then examined using stereo, optical, and transmission electron microscopy (TEM).

For the stereo microscopy analyses, samples were kept in seawater at 2 °C once excised and promptly analyzed under a Discovery V8 stereo microscope with an Axiocam 208 color microscope objective (Carl Zeiss Microscopy GmbH, Germany). Images were processed with AxioVision software (verison 4.7.2, AxioVision, Zeiss, Italy), and the brightness and contrast of images were adjusted using Adobe Photoshop (version 23.2.1, Adobe Systems, USA). Additionally, analysis and observations specifically focused on counting the number of melanophores present in silver, golden, and black tissue samples were performed by subdividing the images taken with zoom 30 x, in 604^2 pixel (equivalent to 0.42 cm^2) sub-images and by counting the nuclei of the melanophores (number of pictures = 135; 3 variants (silver, golden and black), $n = 5$ individuals per variant, 3 independent images per individual, 3 subsets of the image). Average number of melanophores in each sub-image was then calculated, and one-way ANOVA, followed by post hoc pairwise comparison tested with Tuckey's test, were used to statistically test for differences in melanophore abundance. The density of the melanophores was calculated by dividing the number of melanophores by the area analyzed (melanophores/cm^2). A similar approach was undertaken for the images (number of pictures = 15; 5 individual (panda), 3 sub-image: golden, edge [½ golden, ½ black], black) at the edge of the black–golden color transition of "panda" barramundi, however the zoom was 20 x, and a 302^2 pixel (equivalent to 0.21 cm^2) sub-image was obtained, to ensure both the golden and black areas were included in the sub-image.

For the optical microscopy, samples were fixed in 10% neutral buffered formalin, dehydrated in ethanol, cleared in xylene, and embedded in paraffin. Sections (2–3 μm) were stained, utilizing standard protocols, with hematoxylin-eosin (H&E) and Masson-Fontana. The slides were then scanned with an automated slide scanner (Aperio LV1 IVD, Leica Microsystems Pty Ltd., Australia). Digitalized images were analyzed with Aperio ImageScope software (version 12.4.0.5043) and Adobe Photoshop 23.2.1.

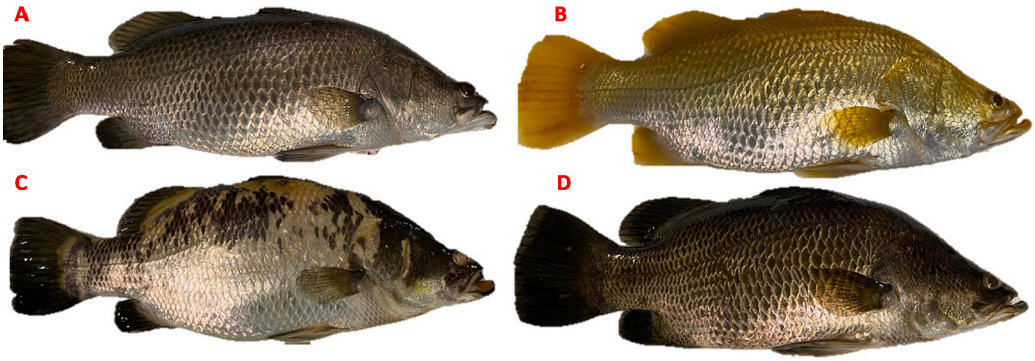

Fig. 1. Multiple skin color phenotypes in *Lates Calcarifer*. A) silver, B) golden, C) panda, D) black.

2.3. Transmission electron microscopy (TEM)

Small samples (approximately 2 mm^2) were taken from ventral skin, dorsal skin, and the dorsal fin from 12 specimens (three individuals from each variant, including silver, golden, panda, and black). Tissue samples were fixed in glutaraldehyde and paraformaldehyde in 0.1 M sodium cacodylate buffer pH 7.4 (ProSciTech Pty Ltd., Australia) and kept at −20 °C. The samples were en bloc stained with 2% aqueous uranyl acetate for 30 min in the dark, then post-stained with 1% osmium tetroxide for 1 h. The samples were dehydrated in a graded series of ethanol/water concentrations and embedded into Epon resin (Embed 812 Kit, EMS). Ultra-thin sections of 70–100 nm of the samples were taken along the longitudinal axis of the fish using a microtome (Ultracut UC7 Leica Microsystem, Austria) and post-stained with lead citrate and uranyl acetate. Specimens were imaged in a transmission electron microscope (H-7800, Hitachi, Japan) operating at 80 kV. Adobe Photoshop software 23.2.1 was used to adjust the brightness and contrast of the images.

2.4. Mc1r – gene and protein characterization, sequence alignment, and antibody choice

Mc1r (melanocortin 1 receptor) is a G protein-coupled receptor, primarily present on melanophores (Feeley and Munyard, 2009), that has been described in several vertebrates, including teleosts (Feeley and Munyard, 2009; Jiang et al., 2021; Metz et al., 2006; Sturm et al., 2001; Takahashi et al., 2016). However, the characterization of the *mc1r* gene was still missing in L. *calcarifer*. Being specific to melanophores, Mc1r detection through immunohistochemistry has been utilized in mammals to determine the presence of these cells in different organs and tissues (Swope et al., 2012). In the present study, Mc1r detection was used to determine the difference in melanophore population between the multiple color variants in the skin of barramundi.

The barramundi *mc1r* gene sequence was first looked for within the barramundi genome (RefSeq: GCF_001640805.1). Initially, the basic local alignment search tool (BLAST) (Altschul et al., 1990) was utilized to search the barramundi genome database utilizing the known zebrafish *mc1r* gene (Gene ID: 353151). Homolog for *mc1r* was identified in the DNA contig (LBLR01010943.1_Lates_calcarifer_10943). Subsequently, BLAST (Altschul et al., 1990), FASTA (Pearson and Lipman, 1988), and the translate tool of Exasy (Gasteiger et al., 2005) were utilized to predict the protein and annotate the gene. The gene organization and predicted amino-acids sequence for *mc1r* used in this investigation were determined for comparison between species. Selected vertebrate *mc1r* sequences - *Takifugu bimaculatus* (TNM91179.1), *Poecilia reticulata* (XP_008403681), *Gambusia affinis* (XP_043993552.1), *Liparis tanakae* (TNN74950.1), *Sebastes umbrosus* (XP_037646789.1), *Sparus aurata* (XP_030270706.1), *Mugil cephalus* (XP_047435784.1), *Perca flavescens* (XP_028434928.1), *Seriola dumerili* (XP_022599193.1), *Seriola lalandi dorsalis* (XP_023251476.1), *Labrus bergylta* (XP_020490269.1), *Morone saxatilis* (XP_035537986.1), *Chelmon rostratus* (XP_041789782.1), *Larimichthys crocea* (XP_010739809.1), *Collichthys lucidus* (TKS70083.1), *Dicentrarchus labrax* (CAY39344.1), *Toxotes jaculatrix* (XP_040905375.1), *Homo sapiens* (Q01726.2), *Mus musculus* (Q01727.2), *Gallus gallus* (P55167.1), *Rana temporaria* (ABU96501.1), *Latimeria chalumnae* (XP_005999265.1) - were retrieved from the NCBI database and multiple sequence alignments of selected amino acid and nucleotide sequences were generated using ClustelX v1.81 (Larkin et al., 2007). Additionally, the protein sequence alignment of human (Q01726.2), mice (Q01727.2), and barramundi Mc1r was compared to identify conserved protein regions (immunogen), targets of commercially available polyclonal antibodies. Importantly, barramundi Mc2r, Mc3r, Mc4r, and Mc5r protein sequences were also predicted and aligned against Mc1r to identify conserved and non-conserved regions. Ultimately, to select the best antibody for this investigation, available Mc1r-specific antibodies were screened utilizing the following parameters: 1) the immunogen was targeting a conserved region (between mice, human, and barramundi) of the Mc1r protein, 2) the immunogen was targeting a non-conserved region between barramundi Mc1r, Mc2r, Mc3r, Mc4r, Mc5r and therefore being specific to Mc1r, without cross-reactivity, 3) the antibody was appliable in immunohistochemistry techniques (paraffin).

The coding cDNA of barramundi *mc1r* (Fig. 2A) was predicted from the L. *calcarifer* genome. The cDNA sequence of *mc1r* was intronless and 972 nucleotides (nt) in length. The barramundi cDNA sequence of *mc1r* encoded for a 324 amino acid protein, with a predicted molecular weight of 36.98 kDA. Alignment of the predicted sequence of barramundi Mc1r protein with selected known vertebrate Mc1r sequences (Supplementary material 1) showed the presence of a number of conserved regions, including the C-terminal tripeptide motif CSW. The barramundi Mc1r, Mc2r, Mc3r, Mc4r, and Mc5r amino acids sequences were also aligned to identify non-conserved regions (data not shown). Additionally, the alignment between barramundi, human, and mice Mc1r was analyzed, and the conserved region was compared with available immunogens of pre-existent commercial antibodies (Fig. 2B).

Following the previously mentioned parameters, an Mc1r specific polyclonal antibody (ThermoFisher Scientific, PA5-21911, RRID: AB_11152789) was chosen for the immunohistochemistry study, whose target is specific for the region between amino acid position 253 and 317 of the homolog human Mc1r protein.

2.5. Immunohistochemistry

The waxed blocks utilized for the histology staining were sent to the QIMR Berghofer Medical Research Institute, Brisbane, Queensland, Australia, for protocol development and immunohistochemistry staining. Sections (3–4 μm) were affixed to positively charged adhesive slides and air-dried overnight at 37 °C. Those were then dewaxed and rehydrated through xylol and descending graded alcohols to water using standard protocols. Endogenous peroxidase activity was blocked by incubating the sections in 1.0% H_2O_2 in TBS (Tris-buffered saline). The sections were washed in three changes of water for 5 min and then washed in three changes of TBST (Tris-buffered saline with 0.1% Tween®) buffer for 5 min. To better visualise the antibody beneath the melanin, an additional step was performed to bleach the melanin in selected slides: melanin pigment in skin and fin tissue was bleached using 0.3% aqueous potassium permanganate and 3.0% aqueous oxalic acid. Antigen retrieval was undertaken using Diva antigen retrieval solution (Biocare Medical, USA) at 100 °C for 20 min using a decloaking chamber. Sections were then washed in three changes of TBST buffer for 5 min each. Nonspecific antibody binding was inhibited by incubating the sections in Background Sniper (Biocare Medical, USA) for 30 min. Primary antibody, rabbit anti-human/anti-mouse Mc1r (AB_11152789) was diluted 1:500 in Da Vinci Green Antibody Diluent (Biocare Medical, USA) and applied on the sections for 60 min at room temperature. The sections were then washed in three changes of TBS_{TW} (Tris-Buffered Saline with Detergent) for 5 min each, and MACH2 Rabbit Polymer HRP was applied for 30 min. Sections were then washed in three changes of TBS_{TW}. Control slide signals were developed in Nova Red for 5–10 min and counterstained in Hematoxylin. The slides were subsequently scanned with an automated slide scanner (Aperio LV1 IVD, Leica Microsystems Pty Ltd., Australia). Digitalized images were analyzed with Aperio ImageScope software (version 12.4.0.5043) and Adobe Photoshop 23.2.1.

3. Results

3.1. General skin structure and differences in wild-type dorsal/ventral skin

In the epidermis, just above the basal layer, epithelial cells were cubical. In contrast, the middle of the epidermis showed columnar shape epithelial cells, and in the upper region, the epithelial cells had a

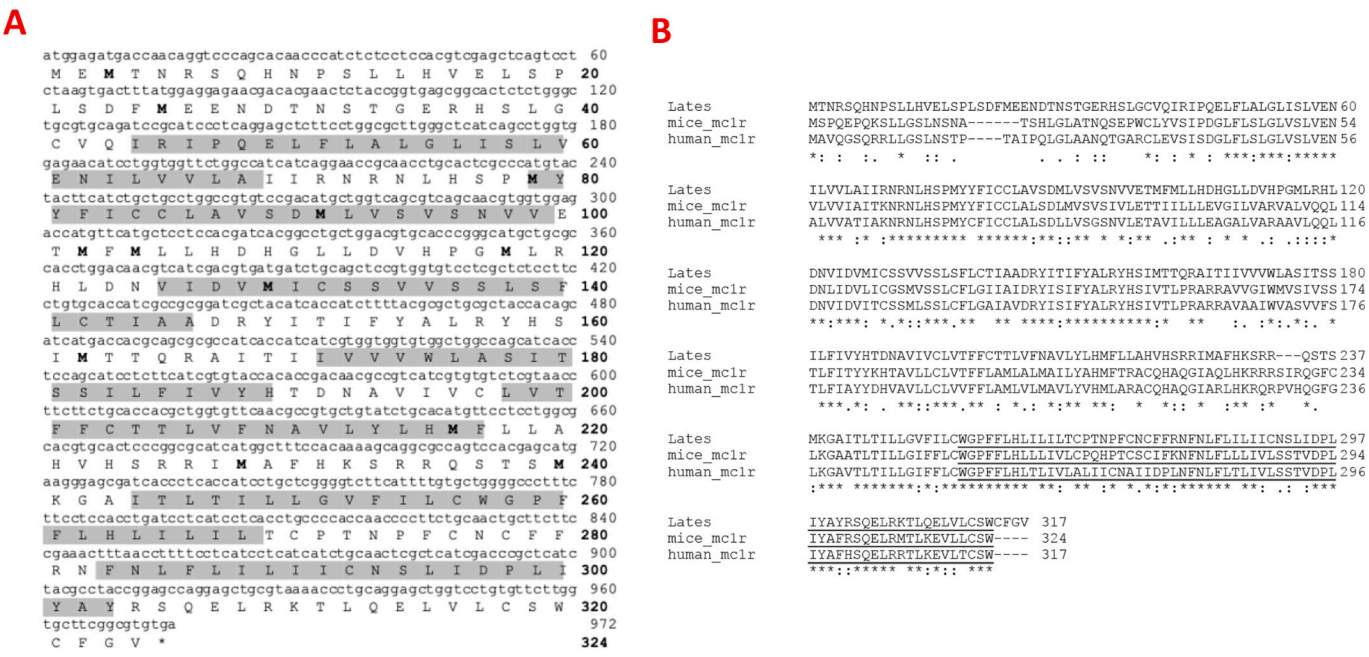

Fig. 2. A: Nucleotides and amino acid sequence of *Lates calcarifer* Mc1r. Highlighted in grey is the intra-membrane region of the receptor. The stop codon was labelled with an asterisk. B: Multiple alignments of the predicted barramundi Mc1r translations with human and mice Mc1r sequences. Identical (*) and similar (: or.) residuals identified by ClustelX program are indicated. Underlined is the region targeted by the selected antibody (RRID: AB_11152789).

flattened morphology (Fig. 3C). The dermis was divided into two distinct layers, the loose connective tissue, the *stratus spongiosum* and the dense collagen tissue, the *stratum compactum*. The loose connective tissue was characterized by collagen and reticulin fibers, while the dense connective tissue was composed of dense and compact collagen fibers, with parallel orientation to the skin surface. The hypodermis was mainly constituted by loose connective tissue with a high number of adipocytes (Fig. 3). The hypodermis was lying above and in some areas within the muscle tissue.

Between the dorsal and ventral skin of silver barramundi, there was an evident difference in cell pigment density and structure. With the utilization of the Masson-Fontana stain, specific to melanin, it was possible to highlight the presence of pigment in the epidermis, both layers (*stratus spongiosum* and *stratum compactum*) of the dermis, and the hypodermis of the dorsal skin (Fig. 3D). In contrast, the ventral skin appeared to have no melanin in the dermis and hypodermis, while the presence of melanin was rarely observed in the epidermis. Instead, iridophores with filament-like, brown pigment layers were detected in both layers of the dermis (Fig. 3E). Also, through the H&M staining technique, xanthophores in the dorsal skin were detected. In fact, a light yellow/brown pigment layer was present in the epidermis underneath the melanin.

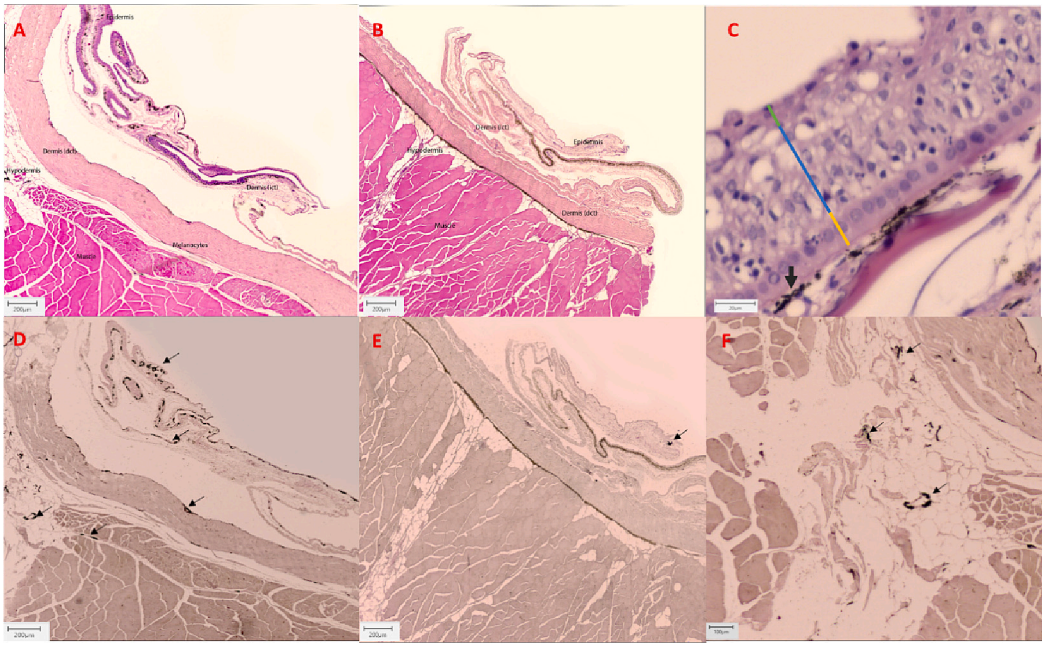

Fig. 3. Histological analysis of wild-type silver barramundi with (A, B. C) H&E stain and (D, E, F) Masson-Fontana stain. A and D: dorsal skin; B and E: ventral skin. C: different cell layers in the epidermis (green: flattened cells, blue: columnar shape cells, and yellow: cubical cells). F: features the hypodermis of dorsal skin with the presence of melanin. Black arrows indicate melanin. (For interpretation of the references to color in this figure legend, the reader is referred to the web version of this article.)

3.2. Pigment differences in the dorsal skin of color variants

Similar to what was seen in silver barramundi through the H&M staining, a clear layer of xanthophores was observed underneath the epidermis cubical cells in all samples of golden, panda, and black barramundi. However, substantial differences in the presence and density of melanophores expressing melanin were observed between the dorsal skin samples of color variants (Fig. 4 and 4G). In particular, in all the golden barramundi samples, no melanin was evidently present in the epidermis, dermis, hypodermis, or muscle tissue (Fig. 4A). However, in 80% of the samples analyzed from golden, panda and black barramundi, nests of melanophores expressing melanin were observed in the hypodermis (Fig. 4D and G). Additionally, within the skin of panda barramundi, the golden patches followed the skin structure of golden individuals (Fig. 4A and G), with no presence of melanin in the epidermis or dermis. However, within the black patches, there was presence of melanophores producing melanin in the epidermis and the *stratus spongiosum*, while no melanin was observed in the *stratum compactum*, hypodermis, or muscle tissue (Fig. 4B, E and G). For black barramundi, the skin structure followed that observed in silver barramundi (Fig. 4C, F and G), with melanophores producing melanin present in the epidermis, both dermis layers and hypodermis.

3.3. Pigment layering in the fin of silver, golden, panda, and black barramundi

Dorsal fins of silver, golden, panda, and black barramundi were observed under the stereo microscope (Fig. 5). Fins from silver barramundi were characterized by a high number of melanophores ($\bar{x} = 91.8 \pm 5.2$ melanophores in 604^2 pixel section, equivalent to a density of approximately 218.6 melanophores/cm^2), organized in dendritic, star-like shape. Moreover, a sparse number of contracted xanthophores were embedded deeper in the fin epidermis under the melanophores (Fig. 5C). Within the dorsal fins of golden barramundi, however contracted and enlarged xanthophore cells were observed, and very few melanophores were observed ($\bar{x} = 0.2 \pm 0.1$ melanophores in a 604^2 pixel picture, equivalent to a density approximately 0.47 melanophores/cm^2) (Fig. 5C). The analysis revealed a significant main difference between the number of melanophores observed in the black, silver and golden variances ($F(2, 444) = 14{,}609$, $p < 0.001$). Post hoc pairwise comparison using Tuckey's test indicated that statistical significance was observed in the number of melanophores counted between golden vs black ($p < 0.001$), golden vs silver ($p < 0.001$) and silver vs black ($p < 0.001$). As previously described, the panda barramundi variant is characterized by a variable pattern of dark (silver/black) and golden patches. To better appreciate the differences between the two-color patches of the fish, fin tissues at the edge between the color change were analyzed. The initial ANOVA analysis revealed a significant main difference between black, edge and golden in the panda barramundi, $F(2,42) = 904.1$, $p < 0.001$). Post hoc comparison using Tuckey's test indicated that there was a clear and statistically significant decrease in the presence of melanophores from the golden ($\bar{x} = 14.2 \pm 1.7$ per 302^2 pixel, equivalent to approximately 67.61 melanophores/cm^2), edge ($\bar{x} = 91.4 \pm 3.5$ per 302^2 pixel, equivalent to approximately 435 melanophores/cm^2) to the dark ($\bar{x} = 138.2 \pm 4.5$ per 302^2 pixel, equivalent to approximately 657 melanophores/cm^2) patches were evident in the following comparisons: golden vs. edge ($p < 0.001$), golden vs. black ($p < 0.001$), edge vs. black ($p < 0.001$) (Fig. 5E). Additionally, dotted (no

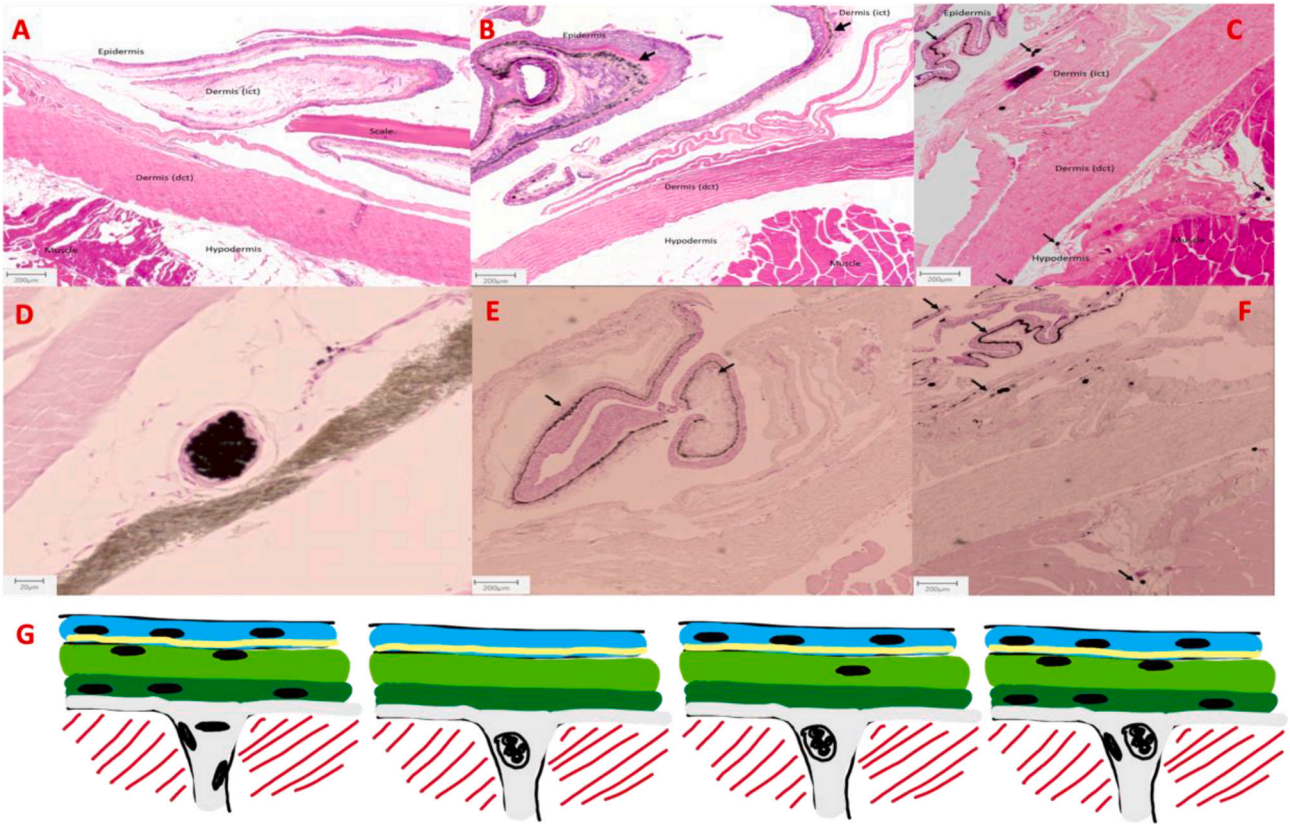

Fig. 4. Histological analysis of dorsal skin of golden (A, D), panda (B, E), and black (C, F) barramundi with (A, B. C) H&E stain and (D, E, F) Masson-Fontana stain. D: nest of melanophores observed in the hypodermis of golden barramundi. Black arrows indicate melanin. G: schematic graph describing the pigment structure in the dorsal skin of color variants, left to right: silver, golden, black patches of panda, black. Blue: epidermis, light green: loose connective tissue, dark green: dense connective tissue, grey: hypodermis, red stripes: muscle; yellow layer representing xanthophores and black ovals representing melanin. (For interpretation of the references to color in this figure legend, the reader is referred to the web version of this article.)

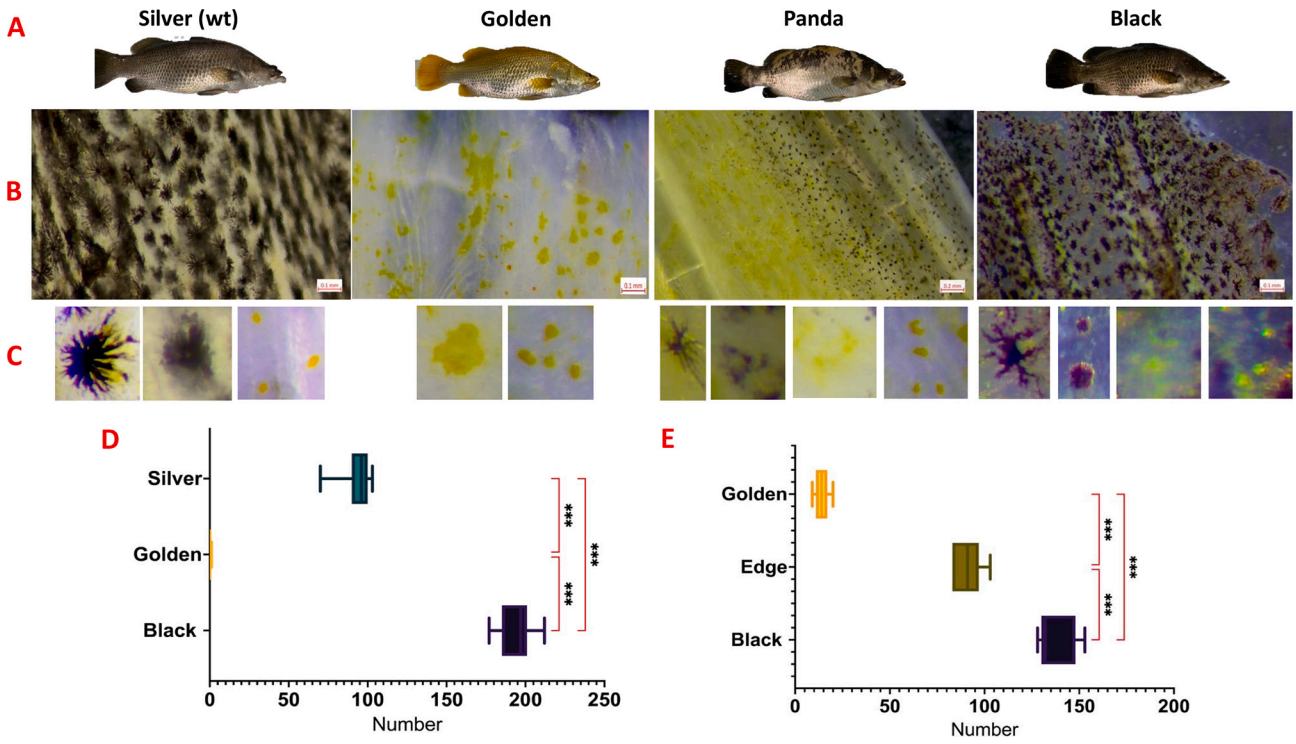

Fig. 5. A: different barramundi color variants. B: Silver, golden, panda, and black dorsal fin of barramundi were analyzed under the stereo microscope, and the evident differences in pigment cell density and presence. C: pigment cells observed with the stereo microscope (Magnification: 80×). D: Boxplot representing the melanophore number (x axis) between black, golden, and silver color variants (604^2 pixel images). E: Boxplot indicating the number of melanophores (x axis) in the panda transition between black, edge and golden patch of panda barramundi (302^2 pixel images). In the y axis the gradient bar represents the color transition from black (bottom), to edge (middle), to golden (top). Bars indicate standard error. Pairwise comparison performed with Tukey's test, *** indicating $p < 0.001$.

presence of dendrites) and dendritic melanophores, as well as contracted and enlarged xanthophores, were observed in fin tissue of panda barramundi (Fig. 5C). In the dorsal fin sample of black barramundi, there was a high concentration of both melanophores (dotted and dendritic) ($\bar{x} = 194.4 \pm 5.4$ melanophore per 604^2 pixel section, equivalent to a density of approximately 462.9 melanophores/cm^2) (Fig. 5D), as well as xanthophores (contracted and enlarged). Interestingly, there is a significant difference between the number of melanophores observed in the golden (0.47 melanophores/cm^2) and black (462.9 melanophores/cm^2) fish, $p < 0.001$).

3.4. Ultrastructure of barramundi skin

Transition electron microscopy was utilized to characterize the ultrastructure of the silver, golden and panda variants of barramundi skin and fin. From the silver barramundi scans, the presence of xanthophores and melanophores was confirmed and numerous melanosomes containing melanin were identified in the cytoplasm of the melanophores (Fig. 6A). The melanophores possess a double membrane, and clear differences in the electrodensity of the melanosomes were observed, indicating different stages of melanin maturation. Stage 1, 2, 3, and 4 melanosomes were visually apparent. However, there were differences in grey shades (Fig. 6C). The nucleus of the melanophores was characterized by a round to an oval shape, with apparent dense chromatin. A high number of xanthophores were also observed adjacent to the melanophores. In the golden barramundi, no melanophores with mature melanosomes (stage 2, 3, and 4) were observed (Fig. 6B). However, a small number of melanophores with stage 1 melanosomes were present (Fig. 6D). Golden patches of the panda barramundi followed the TEM structure of golden fish tissue, while black patches followed the structure of silver fish skin as described above.

3.5. Immunohistochemistry

Immunohistological tagging of cells using an anti-Mc1r antibody revealed clear differences in the presence of melanophores in the tissues analyzed. In silver barramundi melanophores with Mc1r protein was detected in both dorsal skin and fin (Fig. 7A and B), while a drastic reduction of immunostained melanophores was evident in the ventral skin. Specifically, in the dorsal skin, melanophores producing melanin were detected in the epidermis, dermis, and hypodermis. In contrast, infrequent observation of melanophores (both producing and non-producing melanin) was identified in the epidermis of the ventral skin. By comparing the same tissue in bleached and normally stained slides, the antibody anti-Mc1r was detectable beneath the melanin, confirming that melanophores are responsible for melanin production in silver barramundi.

In the skin and fin of golden barramundi, a strong reduction of cells tagged through Mc1r immunostaining was evident, with only sparse anti-Mc1r immunostaining of cells observed in the epidermis (Fig. 7C). Interestingly, in the dorsal skin, loose, compact and walled agglomerates of cells with low-melanin production, positive to immunostaining, were also discovered in the dermis of all samples analyzed (Fig. 7D). Additionally, a small number of small, walled melanin-producing cell granulomas (i.e. nested melanin) were visible (Figs. 4D and 7E). When the bleached melanin slides were compared to the normal staining, the antibody anti-Mc1r was detectable beneath the visible melanin (Fig. 7F).

Similar to the golden variants, in the golden patches of panda barramundi, the antibody anti-Mc1r revealed low levels of non-producing melanin melanophores in the upper layers of the skin, while melanin-producing granulomas were present in the hypodermis. In contrast, in the black patches of panda barramundi, anti-Mc1r was tagged to melanophores producing melanin in the epidermis and upper dermis, while no cells tagged by the Mc1r antibody were detected in the lower layers of the skin, with the exception of rare granulomas with

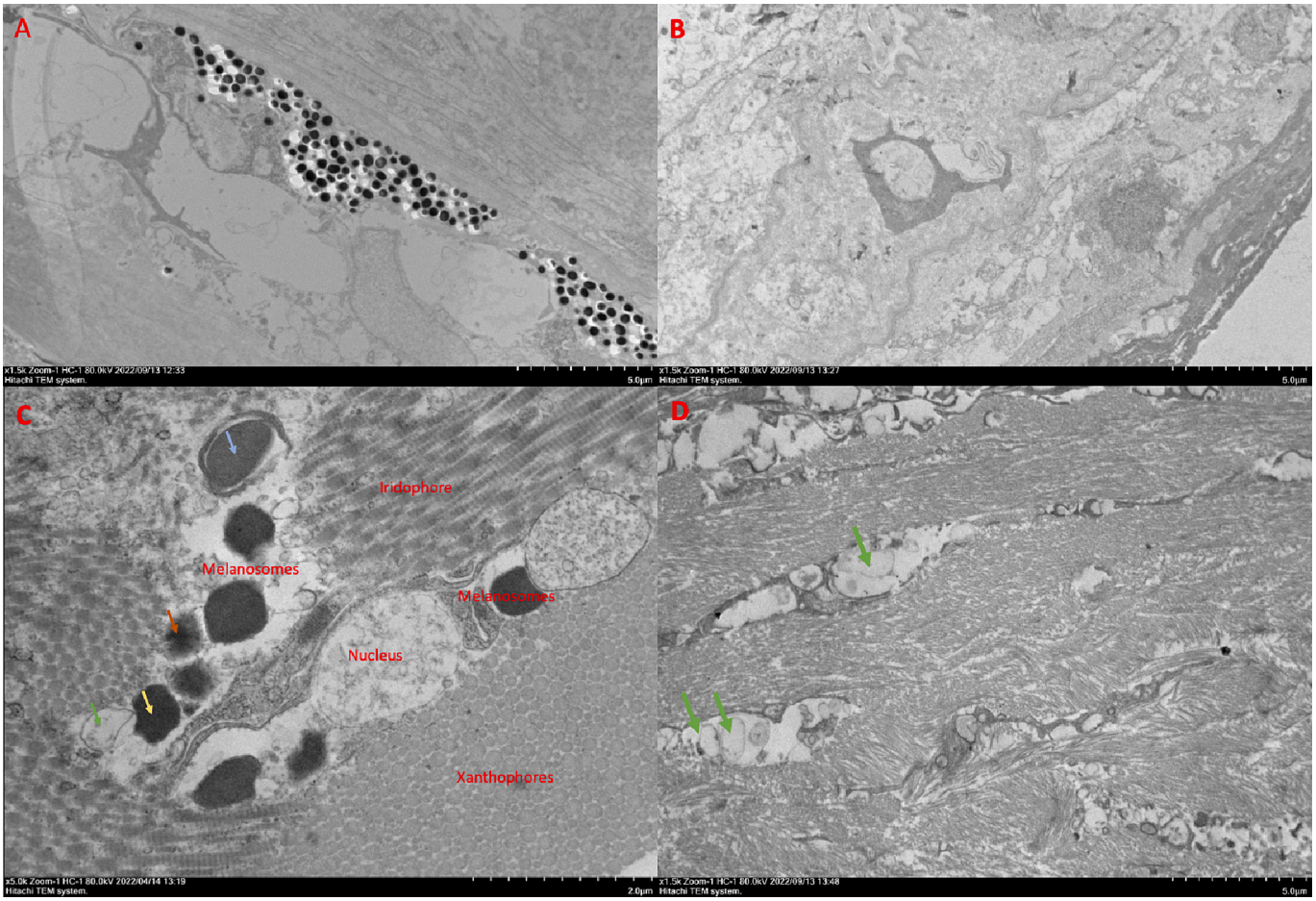

Fig. 6. Skin sample processed with transmission electron microscopy (TEM). A and C represent skin tissues from silver barramundi, and B and D from golden barramundi. A: Evident melanosomes with melanin deposit in silver barramundi fin. B: No evident presence of melanosomes with melanin deposit in golden barramundi fin. C: Evident presence of xanthophores, melanophore with its nucleus and melanosomes, endoplasmic reticulum (yellow arrow: indicating stage 4, blue arrow indicating stage 3, orange arrow indicating stage 2 and green arrow indicating stage 1). D: golden barramundi fin with melanosomes at stage 1 (green arrow). (For interpretation of the references to color in this figure legend, the reader is referred to the web version of this article.)

melanin-producing melanophores. Black and silver barramundi were similar, with Mc1r detection particularly visible after melanin bleaching in all layers of the skin, including the hypodermis. Noticeably, also in black barramundi, small, rare granulomas were visible in the hypodermis.

4. Discussion

The aim of this investigation was to a) understand the differences in skin structure and cell composition between the phenotypic color variants observed in L. *calcarifer*, and b) describe the main morphological features of the skin of this species at a histological and ultrastructural level. Additionally, the presence of melanophores was investigated with immunohistochemistry techniques, through the detection of Mc1r protein receptor, with an anti-Mc1r polyclonal antibody.

Until the present study, there have been only brief descriptions of barramundi skin structure with regards to the effect of infectious disease on skin health (Gibson-Kueh, 2012; Trujillo-González et al., 2015). No studies have described the presence and distribution of pigment cells, particularly, melanophores. However, evidence of melanin in barramundi skin is visible in previously published histological images (Hender et al., 2021), showing a similar structure to what has been observed in this present investigation. The skin of teleosts has been described widely in multiple finfish species (Cordero et al., 2017; Elliott, 2011; Faílde et al., 2014; Zhang et al., 2022). Although there are inter-species and intra-species differences (Ferguson, 1989), the histological and ultrastructural characteristics of barramundi skin follow the typical teleost type, with the distinct layers of the epidermis, dermis (both loose and dense connective tissue), followed by hypodermis and muscle tissue. No differences were observed in the skin structure of dorsal and ventral skin of barramundi; however, a clear variation in presence/absence of melanin was observed between the two skin regions. Differences in coloration between the dorsal and ventral portion of the barramundi are also visually evident, with the dorsal part of the animal being darker shaded than the ventral. Interestingly, this characteristic color pattern, defined as countershading, is evolutionarily conserved in several taxa and not only protects the animal from ultra-violet light, but in aquatic environments also provides an anti-predator cryptic pigmentation (Ruxton et al., 2004). In mammals, the changes in skin and hair color have been associated with a biochemical difference in the melanin production from the melanocytes, with a shift from eumelanin to pheomelanin, regulated through the expression of the gene Agouti-signaling protein (Asip) (Lamoreux et al., 2010). Nevertheless, the presence of pheomelanin in teleosts is still an unanswered question in the literature (Kottler et al., 2015); however, evidence of correlations between the gradual expression of *asip* gene and changes in coloring has been reported in several finfish (Cal et al., 2017; Cal et al., 2019a; Cal et al., 2019b; Liang et al., 2021). Most importantly, it has been demonstrated that the change in color between the dorsal and ventral skin seen in certain finfish species is due to a significant reduction in the number of pigment-producing cells. This contrasts with the biochemical shift in the pigment produced as seen in mammals, with almost no

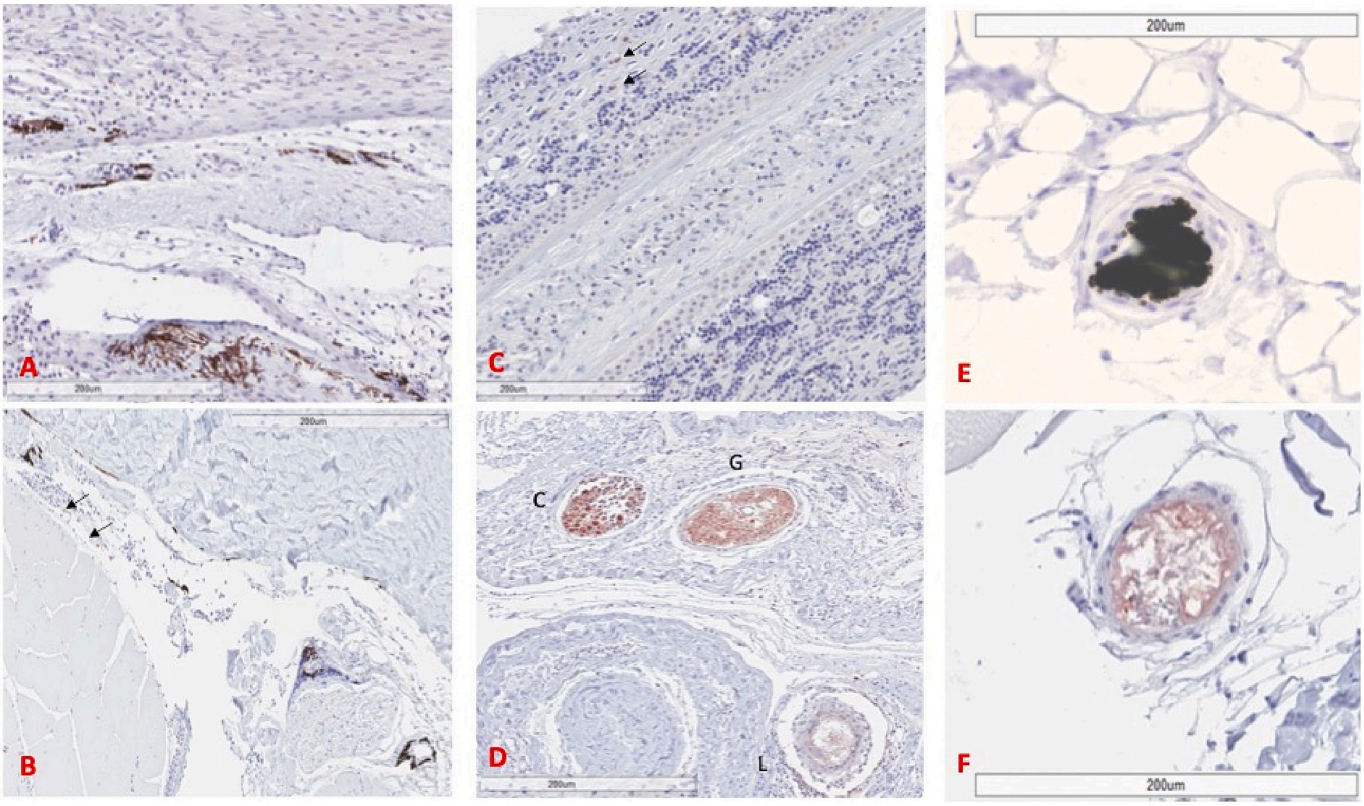

Fig. 7. Immunohistochemistry sections of silver (A, B) and golden (C, D, E, F) barramundi. A, C: dorsal fin, B: hypodermis, D: dermis. E: Unbleached slide with evident small walled granulomas containing melanin. F: Bleached slide with Mc1r immunostaining within the walled granulomas. Arrows indicating Mc1r detection in non-melanin-producing melanophores. C: compact agglomerate of melanophores, L: loose agglomerate of melanophores, G: walled granulomas with melanophores.

presence of melanophores nor xanthophores in the ventral skin (Cal et al., 2019a). From the histological analysis of silver barramundi skin, it was possible to observe a clear difference in the presence of melanin between the dorsal and ventral skin.

Based on histology alone, it was not possible to determine if the absence of melanin was due to a) the non-production of melanin by the melanophores or, b) the absence of melanophores themselves. Through the utilization of a polyclonal antibody for the Mc1r, it was possible to demonstrate that the barramundi countershading is determined by the presence/absence of melanophores. Low numbers of Mc1r were detected in the layers of the ventral skin of the silver barramundi. In contrast, high abundance of Mc1r (and therefore melanophores) was observed within the epidermis, dermis, and hypodermis of the dorsal skin. Additionally, melanophores with melanosomes containing melanin were also identified in the dorsal skin and fin of silver barramundi using TEM. However, melanophores or mature melanosomes were not identified in the golden fish, confirming the patterns observed in the immunohistochemistry analysis. Moreover, the four stages of melanosomes were visible in the silver samples, highlighting the ongoing production of melanin in those tissues (Raposo and Marks, 2007), while only low numbers of observations of stage 1 immature melanosomes were visible in the golden samples.

The ultimate color of the skin is also due to the layering of the pigmented cells, with a vertical order of chromatophores described in multiple finfish species. Interestingly, the characteristic order in which the cells are organized appears to be species-specific. For example, in zebrafish fin, xanthophores are in the uppermost skin layer, iridophores beneath, and melanophores in the basal layer (Hirata et al., 2005); in turbot species, melanophores and xanthophores are in the upper layer, while iridophores are in the basal layer (Faílde et al., 2014). Similarly, the order in the layering of chromatophores in the fin structure of silver barramundi, with melanophores being in the upper layer, xanthophores layering underneath, and iridophores in the basal layer, is conserved. However, the abundance, and in some cases, their presence within the skin layers differed substantially across color variants.

Within the dorsal fins of golden barramundi, no melanin was detected. Similarly, the edge between dark and golden patches of panda variants showed a clear reduction of melanin in the golden color patch compared to adjunct black patches. Changes in pigment cell populations within different color patterns have been extensively reported, with most studies undertaken in zebrafish (Patterson and Parichy, 2019; Singh and Nüsslein-Volhard, 2015). From those, it is clear that cell-cell interactions (Maderspacher and Nüsslein-Volhard, 2003), signaling, and pathways related to melanophore differentiation and survival, with genes involved such as *asip1* and *agrp2*, all play a major role in defining stripes and patch formation (Singh and Nüsslein-Volhard, 2015). Most studies have correlated the changes in color pattern to the different pigment cell populations, specifically the absence of melanophores. However, some studies suggested that the non-production of melanin and aggregation of melanosomes are the causative reason for the lighter color of the skin. This has been observed when the fish is adapting to new backgrounds or responding to stress [13] and in multiple color phenotypes. For example, in green sunfish (*Lepomis cyanellus*), golden variants have been linked to a reduction in the number of melanophores and melanin granules (Dunham and Childers, 1980), rather than a reduction in melanophores. In this present study, clear differences in the quantity of melanin were observed between the multiple color variants of barramundi, with a substantial reduction of melanin within the layers of the skin in the golden variants (both full golden and golden patches of panda). However, using histological analysis, it was not possible to determine if the melanophores were present and not producing melanin, or if they were absent. To answer this, similar to the countershading

characterization, an immunohistochemistry technique was utilized through the detection of the Mc1r protein. In recent years, antibodies targeting proteins involved in melanin production, such as Tyr, Mitfa or Pmel, have been developed and utilized in fish (Chen et al., 2019; Gramann et al., 2019). Yet, although identifying these proteins is informative, utilizing those antibodies was out of the scope of this study as the question was why the skin of golden barramundi lacked apparent melanin. Therefore, targeting a melanophore cell-specific membrane receptor such as Mc1r, involved in the switching on/off of melanin production, would identify if melanophores were actually present and not producing melanin, or absent entirely. In fact, from this investigation, it was observable that in golden barramundi (and in the golden patches of panda barramundi) the presence of Mc1r was drastically reduced, denotating a reduction of melanophore occurrence. Additionally, different stages of aggregation of non-producing melanin melanophores were evident in the dermis, as well as small walled granulomas containing melanin within the hypodermis.

In a broader context, it is essential to clarify that while most of the xanthic phenotypes reported in the literature appear to be due to a stable and heritable trait, the color of barramundi is not. Not only are golden barramundi born silver and subsequently change color, but they can also revert during their lifetime. Observations have revealed that stressful events such as water quality and transport changes can trigger color changes, such as golden and panda reverting to silver/black variants (H. S. Cate, personal communication, March 27, 2022). This suggests that in those individuals the melanophores have the capability to re-produce melanin when triggered. Similar to barramundi, goldfish (*Carassius auratus*) change color (from grey to red) throughout their lifetime, and this transition has been extensively studied (Zhang et al., 2017a, 2017b). Specifically, the transformation from grey to red coloration was characterized by a reduction in the number of melanophores and a significant decrease in melanosomes and melanin production within the remaining pigment cells, showing a similar physiological response to that observed in barramundi. Additionally, apoptosis pathways were highly regulated in the goldfish, with a statistically significant reduction of *mc1r* expression and up regulation of the *asip1* gene (Zhang et al., 2017b). In *PmelA-/PmelB-* engineered golden tilapia (*Oreochromis aureus*), a decrease in melanophore number and sparse melanin-free melanophores were observed in the skin (Wang et al., 2022). Moreover, fish held in tanks with a white background also showed a reduction in the number of melanophores, with just a few surviving long-term adaptation. However, melanophores could re-establish their original size, dendricity and melanin production and proliferate when fish were transferred to tanks with a black background (Sugimoto, 2002). This capability of re-establishing the melanin pathways and multiplication of the non-melanin-producing melanophores after specific triggers could explain the capacity of golden barramundi to revert to black. However, this study not only detected a reduced number of melanophores and a reduced melanin production within the golden phenotype, but it also detected agglomeration of non-melanin-producing melanophores and nested melanin-producing melanophores. Moreover, agglomeration of melanin-producing melanophores in organs, such as the spleen and liver, has been reported as a stress, parasite, and/or immune defense response (Salimi, 2017). This leads to an alternative explanation whereby it could be possible that the color variants have an enhanced response to stress leading to melanophore aggregation and death, resulting in skin color changes. Interestingly, in golden loach (*Paramisgumus dabryanus*), the absence of melanin was observed in the histological analysis (Zhang et al., 2022), but most importantly, pathways associated with immune system response, autoimmune diseases, cytokine-cytokine interaction, and apoptosis were highly upregulated in the golden fish (Huang et al., 2021). Significantly, this could indicate that in loach, the golden coloration could result from multiple physiological changes and molecular interactions rather than simple melanin reduction/melanophore death, similar to what was seen in barramundi.

In this present study, we described the structure and cell pigment populations of silver barramundi and color variants, laying the basis for future investigation. Understanding the genetic basis of the golden phenotype, the abundance, and presence of melanophores, and whether they produce melanin is an important step toward manipulating color and producing higher proportions of golden barramundi within an industrial aquaculture context.

Supplementary data to this article can be found online at https://doi.org/10.1016/j.aquaculture.2023.739859.

Funding

Grant title: Striking Gold - Determining the genetic drivers of gold coloration in barramundi.

Funding body: Australian Research Council (ARC), fund scheme: Linkage.

CRediT authorship contribution statement

R. Marcoli: Conceptualization, Methodology, Validation, Formal analysis, Investigation, Writing – original draft, Visualization, Supervision. **D.B. Jones:** Writing – review & editing, Funding acquisition. **C. Massault:** Writing – review & editing. **M. Moran:** Writing – review & editing. **P.J. Harrison:** Resources, Funding acquisition. **H.S. Cate:** Resources, Funding acquisition. **A.L. Lopata:** Methodology, Supervision. **D.R. Jerry:** Conceptualization, Resources, Supervision, Funding acquisition.

Declaration of Competing Interest

The authors declare the following financial interests/personal relationships which may be considered as potential competing interests:

Roberta Marcoli reports financial support was provided by Australian Research Council.

Data availability

Data will be made available on request.

Acknowledgments

We would like to acknoladge our funding body ARC (Australian Research Council) through the found scheme Linkage, with the grant title: "Striking Gold: Determining the genetic drivers of gold coloration in barramundi", ID: LP200201003. We would also like to acknowledge Jarrod Guppy for his support and help during the sampling collection.

References

Altschul, S.F., Gish, W., Miller, W., Myers, E.W., Lipman, D.J., 1990. Basic local alignment search tool. J. Mol. Biol. 215 (3), 403–410. https://doi.org/10.1016/S0022-2836(05)80360-2.

Burton, D., 2002. The physiology of flatfish chromatophores. Microsc. Res. Tech. 58 (6), 481–487. https://doi.org/10.1002/jemt.10166.

Burton, D., 2011. The Skin| Coloration and Chromatophores in Fishes doi:10.1016/B978-0-12-374553-8.00041-1.

Cal, L., Suarez-Bregua, P., Cerdá-Reverter, J.M., Braasch, I., Rotllant, J., 2017. Fish pigmentation and the melanocortin system. Comp. Biochem. Physiol. 211, 26–33. https://doi.org/10.1016/j.cbpa.2017.06.001.

Cal, L., Suarez-Bregua, P., Comesaña, P., Owen, J., Braasch, I., Kelsh, R., Cerdá-Reverter, J.M., Rotllant, J., 2019a. Countershading in zebrafish results from an Asip1 controlled dorsoventral gradient of pigment cell differentiation. Sci. Rep. 9 (1), 1–13. https://doi.org/10.1038/s41598-019-40251-z.

Cal, L., Suarez-Bregua, P., Braasch, I., Irion, U., Kelsh, R., Cerdá-Reverter, J.M., Rotllant, J., 2019b. Loss-of-function mutations in the melanocortin 1 receptor cause disruption of dorso-ventral countershading in teleost fish. Pigment Cell Melanoma Res. 32 (6), 817–828. https://doi.org/10.1111/pcmr.12806.

Chen, Y.-M., Su, W.-C., Li, C., Shi, Y., Chen, Q.-X., Zheng, J., Tang, D.-L., Chen, S.-M., Wang, Q., 2019. Anti-melanogenesis of novel kojic acid derivatives in B16F10 cells and zebrafish. Int. J. Biol. Macromol. 123, 723–731. https://doi.org/10.1016/j.ijbiomac.2018.11.031.

Colihueque, N., 2010. Genetics of salmonid skin pigmentation: clues and prospects for improving the external appearance of farmed salmonids. Rev. Fish Biol. Fish. 20 (1), 71–86. https://doi.org/10.1007/s11160-009-9121-6.

Cordero, H., Ceballos-Francisco, D., Cuesta, A., Esteban, M.Á., 2017. Dorso-ventral skin characterization of the farmed fish gilthead seabream (*Sparus aurata*). PLoS One 12 (6), e0180438. https://doi.org/10.1371/journal.pone.0180438.

Dong, X., Lei, W., Zhu, X., Han, D., Yang, Y., Xie, S., 2011. Effects of dietary oxidized fish oil on growth performance and skin colour of Chinese longsnout catfish (*Leiocassis longirostris* Günther). Aquac. Nutr. 17 (4), e861–e868. https://doi.org/10.1111/j.1365-2095.2011.00854.x.

Dunham, R.A., Childers, W.F., 1980. Genetics and implications of the golden color morph in green sunfish. Prog. Fish Cult. 42 (3), 160–163. https://doi.org/10.1577/1548-8659(1980)42[160:GAIOTG]2.0.CO;2.

Elliott, D., 2011. The Skin| Functional Morphology of the Integumentary System in Fishes doi:10.1016/B978-0-12-374553-8.00108-8.

Estlander, S., Nurminen, L., Olin, M., Vinni, M., Immonen, S., Rask, M., Ruuhijärvi, J., Horppila, J., Lehtonen, H., 2010. Diet shifts and food selection of perch *Perca fluviatilis* and roach *Rutilus rutilus* in humic lakes of varying water colour. J. Fish Biol. 77 (1), 241–256. https://doi.org/10.1111/j.1095-8649.2010.02682.x.

Faílde, L., Bermúdez, R., Vigliano, F., Coscelli, G.A., Quiroga, M.I., 2014. Morphological, immunohistochemical and ultrastructural characterization of the skin of turbot (*Psetta maxima L.*). Tissue Cell 46 (5), 334–342. https://doi.org/10.1016/j.tice.2014.06.004.

Feeley, N., Munyard, K., 2009. Characterisation of the melanocortin-1 receptor gene in alpaca and identification of possible markers associated with phenotypic variations in colour. Anim. Prod. Sci. 49 (8), 675–681. https://doi.org/10.1071/AN09005.

Ferguson, H.W., 1989. Systemic Pathology of Fish. A Text and Atlas of Comparative Tissue Responses in Diseases of Teleosts. Iowa State University Press.

Gasteiger, E., Hoogland, C., Gattiker, A., Wilkins, M.R., Appel, R.D., Bairoch, A., 2005. Protein identification and analysis tools on the ExPASy server. The Proteomics Protocols Handbook 571–607. https://doi.org/10.1385/1-59259-890-0:571.

Gibson-Kueh, S., 2012. Diseases of Asian Seabass (or Barramundi), *Lates calcarifer* Bloch. Murdoch University.

Gramann, A.K., Venkatesan, A.M., Guerin, M., Ceol, C.J., 2019. Regulation of zebrafish melanocyte development by ligand-dependent BMP signaling. eLife 8, e50047. https://doi.org/10.7554/eLife.50047.

Hender, A., Siddik, M.A.B., Howieson, J., Fotedar, R., 2021. Black soldier Fly, *Hermetia illucens* as an alternative to fishmeal protein and fish oil: impact on growth, immune response, mucosal barrier status, and flesh quality of juvenile barramundi, *Lates calcarifer* (Bloch, 1790). Biology 10 (6), 505. https://doi.org/10.3390/biology10060505.

Hirata, M., Nakamura, K.I., Kondo, S., 2005. Pigment cell distributions in different tissues of the zebrafish, with special reference to the striped pigment pattern. Dev. Dyn. 234 (2), 293–300. https://doi.org/10.1002/dvdy.20513.

Huang, Z.H., Ma, B.H., Guo, X.L., Wang, H.H., Ma, A.J., Sun, Z.B., Wang, Q.M., 2021. Comparative transcriptome analysis of the molecular mechanism underlying the golden red colour in mutant Taiwanese loach. Aquaculture 543, 8. https://doi.org/10.1016/j.aquaculture.2021.736979.

Jerry, D.R., 2013. Biology and Culture of Asian Seabass *Lates calcarifer*. CRC Press.

Jiang, L., Kon, T., Chen, C., Ichikawa, R., Zheng, Q., Pei, L., Takemura, I., Nsobi, L.H., Tabata, H., Pan, H., 2021. Whole-genome sequencing of endangered Zhoushan cattle suggests its origin and the association of MC1R with black coat colour. Sci. Rep. 11 (1), 1–11. https://doi.org/10.1038/s41598-021-96896-2.

Kalinowski, C., Izquierdo, M., Schuchardt, D., Robaina, L., 2007. Dietary supplementation time with shrimp shell meal on red porgy (*Pagrus pagrus*) skin colour and carotenoid concentration. Aquaculture 272 (1–4), 451–457. https://doi.org/10.1016/j.aquaculture.2007.06.008.

Kelsh, R.N., 2004. Genetics and evolution of pigment patterns in fish. Pigment Cell Res. 17 (4), 326–336. https://doi.org/10.1111/j.1600-0749.2004.00174.x.

Kottler, V.A., Künstner, A., Schartl, M., 2015. Pheomelanin in fish? Pigment Cell Melanoma Res. 28 (3), 355–356. https://doi.org/10.1111/pcmr.12359.

Lamoreux, M.L., Delmas, V., Larue, L., Bennett, D., 2010. The Colors of Mice: A Model Genetic Network. John Wiley & Sons.

Larkin, M.A., Blackshields, G., Brown, N.P., Chenna, R., McGettigan, P.A., McWilliam, H., Valentin, F., Wallace, I.M., Wilm, A., Lopez, R., Thompson, J.D., Gibson, T.J., Higgins, D.G., 2007. Clustal W and Clustal X version 2.0. Bioinformatics 23 (21), 2947–2948. https://doi.org/10.1093/bioinformatics/btm404.

Leclercq, E., Taylor, J.F., Migaud, H., 2010. Morphological skin colour changes in teleosts. Fish Fish. 11 (2), 159–193. https://doi.org/10.1111/j.1467-2979.2009.00346.x.

Lewand, K.O., Hyde, J.R., Buonaccorsi, V.P., Lea, R.N., 2013. Orange coloration in a black-and-yellow rockfish (*Sebastes chrysomelas*) from Central California. Calif. Fish Game 99 (4), 237–239.

Liang, Y., Grauvogl, M., Meyer, A., Kratochwil, C.F., 2021. Functional conservation and divergence of color-pattern-related agouti family genes in teleost fishes. J. Exp. Zool. B Mol. Dev. Evol. 336 (5), 443–450. https://doi.org/10.1002/jez.b.23041.

Maderspacher, F., Nüsslein-Volhard, C., 2003. Formation of the adult pigment pattern in zebrafish requires leopard and obelix dependent cell interactions doi:10.1242/dev.00519.

Metz, J.R., Peters, J.J., Flik, G., 2006. Molecular biology and physiology of the melanocortin system in fish: a review. Gen. Comp. Endocrinol. 148 (2), 150–162. https://doi.org/10.1016/j.ygcen.2006.03.001.

Nilsson Sköld, H., Aspengren, S., Wallin, M., 2013. Rapid color change in fish and amphibians–function, regulation, and emerging applications. Pigment Cell Melanoma Res. 26 (1), 29–38. https://doi.org/10.1111/pcmr.12040.

Pathan, T., 2022. Novel xanthic phenotype of the silver carp, *Hypothalamichthyes molitrix* (Valenciennes, 1844) identification and characterization. J. Fish Res. 6 (3), 111. https://doi.org/10.35841/2529-8046-6.3.111.

Patterson, L.B., Parichy, D.M., 2019. Zebrafish pigment pattern formation: insights into the development and evolution of adult form. Annu. Rev. Genet. 53, 505–530. https://doi.org/10.1146/annurev-genet-112618-043741.

Pawar, R.T., Jawad, L.A., 2017. First report of A xanthic phenotype of the silver carp, *Hypothalamichthyes molitrix* (Valenciennes, 1844) (Teleostei: Cyprinidae) from Maharashtra fish seed production Centre, India. Aquac. Int. 7 https://doi.org/10.5376/ija.2017.07.0015.

Pearson, W.R., Lipman, D.J., 1988. Improved tools for biological sequence comparison. Proc. Natl. Acad. Sci. 85 (8), 2444–2448. https://doi.org/10.1002/jemt.10166.

Raposo, G., Marks, M.S., 2007. Melanosomes—dark organelles enlighten endosomal membrane transport. Nat. Rev. Mol. Cell Biol. 8 (10), 786–797. https://doi.org/10.1038/nrm2258.

Ruxton, G.D., Speed, M.P., Kelly, D.J., 2004. What, if anything, is the adaptive function of countershading? Anim. Behav. 68 (3), 445–451. https://doi.org/10.1016/j.anbehav.2003.12.009.

Salimi, B., 2017. Histopathology of leech parasitism on *Capoeta capoeta gracilis*, *Squalius cephalus and Carassius auratus*. J. Fish Dis. 30 (2), 97–105. https://doi.org/10.7847/jfp.2017.30.2.097.

Segade, Á., Robaina, L., Otero-Ferrer, F., García Romero, J., Molina Domínguez, L., 2015. Effects of the diet on seahorse (*Hippocampus hippocampus*) growth, body colour and biochemical composition. Aquac. Nutr. 21 (6), 807–813. https://doi.org/10.1111/anu.12202.

Singh, Ajeet P., Nüsslein-Volhard, C., 2015. Zebrafish stripes as a model for vertebrate colour pattern formation. Curr. Biol. 25 (2), R81–R92. https://doi.org/10.1016/j.cub.2014.11.013.

Sturm, R.A., Teasdale, R.D., Box, N.F., 2001. Human pigmentation genes: identification, structure and consequences of polymorphic variation. Gene 277 (1–2), 49–62. https://doi.org/10.1016/s0378-1119(01)00694-1.

Sugimoto, M., 2002. Morphological color changes in fish: regulation of pigment cell density and morphology. Microsc. Res. Tech. 58 (6), 496–503. https://doi.org/10.1002/jemt.10168.

Swope, V.B., Jameson, J.A., McFarland, K.L., Supp, D.M., Miller, W.E., McGraw, D.W., Patel, M.A., Nix, M.A., Millhauser, G.L., Babcock, G.F., 2012. Defining MC1R regulation in human melanocytes by its agonist α-melanocortin and antagonists agouti signaling protein and β-defensin 3. J. Invest. Dermatol. 132 (9), 2255–2262. https://doi.org/10.1038/jid.2012.135.

Takahashi, A., Davis, P., Reinick, C., Mizusawa, K., Sakamoto, T., Dores, R.M., 2016. Characterization of melanocortin receptors from stingray *Dasyatis akajei*, a cartilaginous fish. Gen. Comp. Endocrinol. 232, 115–124. https://doi.org/10.1016/j.ygcen.2016.03.030.

Trujillo-González, A., Johnson, L., Constantinoiu, C., Hutson, K., 2015. Histopathology associated with haptor attachment of the ectoparasitic monogenean *Neobenedenia* sp. (Capsalidae) to barramundi, *Lates calcarifer* (Bloch). J. Fish Dis. 38 (12), 1063–1067. https://doi.org/10.1111/jfd.12320.

Wang, C.X., Xu, J., Kocher, T.D., Li, M.H., Wang, D.S., 2022. CRISPR knockouts of pmela and pmelb engineered a golden tilapia by regulating relative pigment cell abundance. J. Hered. 113 (4), 398–413. https://doi.org/10.1093/jhered/esac018.

Zhang, Y., Liu, J., Fu, W., Xu, W., Zhang, H., Chen, S., Liu, W., Peng, L., Xiao, Y., 2017a. Comparative transcriptome and DNA methylation analyses of the molecular mechanisms underlying skin color variations in Crucian carp (*Carassius carassius L.*). BMC Genet. 18 (1), 1–12. https://doi.org/10.1186/s12863-017-0564-9.

Zhang, Y.Q., Liu, J.H., Peng, L.Y., Ren, L., Zhang, H.Q., Zou, L.J., Liu, W.B., Xiao, Y.M., 2017b. Comparative transcriptome analysis of molecular mechanism underlying gray-to-red body color formation in red crucian carp (*Carassius auratus*, red var.). Fish Physiol. Biochem. 43 (5), 1387–1398. https://doi.org/10.1007/s10695-017-0379-7.

Zhang, Y.B., Wang, T.Z., Zhang, X.Y., Wei, Y.L., Chen, P.Y., Zhang, S.D., Guo, Z.G., Xiong, Y.L., Jiang, J., Huang, X.L., Chen, D.F., Yang, S.Y., Luo, W., Du, Z.J., 2022. Observation of body colour formation and pigment cells in grey-black and golden *Paramisgumus dabryanus*. Aquac. Res. 53 (7), 2657–2669. https://doi.org/10.1111/are.15782.